A Full Order Sensorless Control Adaptive Observer for Doubly-Fed Induction Generator

G. Brando*, A. Dannier*, and I. Spina*
*University of Naples FEDERICO II - Department of Electrical Engineering and Information Technologies, Via Claudio 21, 80125 Napoli, (*Italy*)

***Abstract* — This paper presents a sensorless control for a Doubly Fed Induction Generator (DFIG) in the context of grid-connected turbine-based wind generation systems. The paper proposes a full order adaptive observer able to track with excellent accuracy the DFIG rotor position even in presence of significant parameters deviations. The developed adaptive observer is coupled with a traditional stator flux based Field Oriented Control (FOC). The novel approach has been validated by an extensive numerical analysis.**

***Index Terms* -- doubly-fed induction generator, wind power system, sensorless control, full order observer, field oriented control.**

I. Nomenclature

$\mathbf{i}_s / \mathbf{i}_r$	Space vector of the stator/rotor current
$L_{\sigma s} / L_{\sigma r}$	Stator/rotor leakage inductance
L_m	Air-gap linkage inductance
L_s	Stator inductance $L_s = L_{\sigma s} + L_m$
L_r	Rotor inductance $L_r = L_{\sigma r} + L_m$
R_s / R_r	Stator/rotor resistance
$\mathbf{v}_s / \mathbf{v}_r$	Space vector of the stator/rotor voltage
$\vartheta_r / \vartheta_e$	Mechanical/electrical rotor position
$\mathbf{\Phi}_s / \mathbf{\Phi}_r$	Space vector of the stator/rotor flux
ω_r / ω	Rotor angular speed/angular frequency
^	Superscript to indicate estimated quantity
*	Superscript to indicate reference quantity
(r)	Superscript to indicate rotor reference frame

II. Introduction

The spread of wind-based generation power systems [1] has attracted great interest for the Doubly-Fed Induction Generator (DFIG). The wind generation system must be able to operate in a wide wind speed range in order to ensure optimal aerodynamic efficiency by tracking the best tip-speed ratio, hence extracting the maximum available power. Therefore, the electric generator operates with a variable rotor speed; typically ±35% around the synchronous speed.

In grid-connected systems, currently the most widespread, the stator windings of DFIG are directly supplied by the grid, while a three-phase double stage AC/DC-DC/AC converter feeds the rotor via slip-rings. In this configuration, the major portion of the mechanical power at the shaft is directly transformed to electrical power and supplied to the grid without involving the rotor. Additionally, also the magnetizing current is directly absorbed by the grid. As a consequence, only a fraction of the total power has to be handled by means of the power converter, introducing significant advantages. Indeed, the converter rated power is typically about 30% of the target power generator, resulting a reduction of the initial and operative cost of the system. Moreover, the losses in the power electronic converter is reduced compared to a system where the converter has to handle the whole power.

Differently than for conventional induction machine, the DFIG stator power is conditioned to the rotor voltages. Hence, the driving of the system requires the detection of the rotor position, which is necessary for the transformation from the rotor to the stator reference frame. The usage of position sensors is not advisable against the possible event of failure, especially in stormy weather, where DFIG is employed, invalidating the characteristic of the generator robustness. Actually, this type of generator intrinsically suggests the adoption of a sensorless control. Indeed, the requirement to use additional current transducers, indispensable for monitoring the rotor currents, involves the need to reduce the costs of the other devices of the control system and therefore practically imposes a sensorless control [2],[3].

Different approaches have been proposed in order to realize sensorless control for a variable speed-constant frequency generation system based on a doubly fed induction generator: closed loop estimation [4],[5], Kalman filter [6], high frequency signal injection [7],[8], Model Reference Adaptive System (MRAS) [9],[10] with full or reduced order approaches [11]-[13], etc. In each of these controls, the challenge is to assess the position of the rotor in an indirect way, while keeping a good estimation accuracy against possible parameter deviations.

Depending on the implemented control strategy, such as Field Oriented Control (FOC), Direct Torque Control (DTC) [14]-[16], Direct Power Control (DPC) [17],[18] and so on, it is possible to obtain many different performances, all substantially linked to the opportunity to improve the estimation of the rotor position.

This work proposes a novel adaptive full order observer, proving the estimation of the rotor position to a FOC control scheme. Differently than for other

978-1-7281-1356-2/19/$31.00 ©2019 IEEE

approaches, the rotor position estimation error is not minimized but, instead, regarded as an additional machine parameter. This parameter is precisely tracked by the proposed adaptive law, allowing a quasi perfect compensation of the projection error from the rotor frame to the stator frame.

As testified by numerical investigation, the proposed control is resilient to parametric errors, showing good performance, even in presence of up to ±20% of parameter deviations.

III. Description of the System

A Doubly Fed Induction Generator (DFIG) consists of a wound rotor equipped with slip rings where the stator windings are directly connected to the three-phase grid. Usually, the rotor windings are connected to a back-to-back power converter partially rated (30% of the rating power of the whole system) as shown in Fig. 1.

In particular, the back-to-back converter is a bi-directional power converter consisting of two converter and a common DC-link: Rotor Side Converter (RSC) and Grid Side Converter (GSC) respectively. Due to the bi-directional power flow ability of the converter, the DFIG may operate as a generator or motor in both sub-synchronously and super-synchronously. Indeed in the generator mode operation, the frequency of the RSC is imposed in order to ensure that the frequency AC grid is constant.

The bi-directional converter ensure the capability of the DFIG to operate in sub-synchronous and super-synchronous modes. These two modes are limited in 1/3 up and down of synchronous speed.

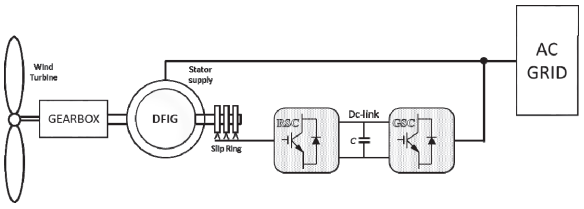

Fig. 1. System block scheme

IV. Proposed Adaptive Observer

The well-known mathematical model of the DFIG can be conveniently presented in its matrix form with respect to the stator reference frame:

$$\frac{\mathrm{d}}{\mathrm{d}t}\begin{bmatrix}\mathbf{i}_s\\ \boldsymbol{\Phi}_s\end{bmatrix}=\begin{bmatrix}A_{11} & A_{12}\\ A_{21} & A_{22}\end{bmatrix}\begin{bmatrix}\mathbf{i}_s\\ \boldsymbol{\Phi}_s\end{bmatrix}+\begin{bmatrix}B_1\\ B_2\end{bmatrix}[\mathbf{v}_s]+\begin{bmatrix}C_1\\ C_2\end{bmatrix}[\mathbf{v}_r] \quad (1)$$

It can be noted that the dynamical equations of a traditional induction machine can be quickly derived from (1) by imposing $\mathbf{v}_r = 0$.

Since all the system state variables and inputs have been defined as space vectors, all the corresponding matrix elements are complex numbers. In particular:

$$\begin{cases} A_{11} = -\left(\dfrac{R_s}{L_{s,eq}} + f_{r,eq}\right) + jp\omega_r \\ A_{12} = \dfrac{\sigma f_{r,eq}}{L_{s,eq}} - j\dfrac{p\omega_r}{L_{s,eq}} \\ A_{21} = -R_s \\ A_{22} = 0 \end{cases} \qquad \begin{cases} B_1 = \dfrac{1}{L_{s,eq}} \begin{cases} C_1 = -\dfrac{B_1}{\mu_r} \\ C_2 = 0 \end{cases} \\ B_2 = 1 \end{cases} \quad (2)$$

where:

$$\mu_r = \frac{L_m}{L_r};\quad \sigma = (1-\mu_s\mu_r);\quad L_{s,eq} = \sigma L_s;\quad f_{r,eq} = \frac{R_r}{L_{r,eq}} \quad (3)$$

with $\mu_s = L_m / L_r$ and $L_{r,eq} = \sigma L_r$.

The space vector of the rotor currents can be easily computed starting from the chosen state variables through the relation:

$$\mathbf{i}_r = \frac{\boldsymbol{\Phi}_s}{L_m} - \frac{L_s}{L_m}\mathbf{i}_s \quad (4)$$

With reference to the DFIG mathematical model (1), a full order Luenberger observer can be defined as:

$$\frac{\mathrm{d}}{\mathrm{d}t}\begin{bmatrix}\hat{\mathbf{i}}_s\\ \hat{\boldsymbol{\Phi}}_s\end{bmatrix} = A\begin{bmatrix}\hat{\mathbf{i}}_s\\ \hat{\boldsymbol{\Phi}}_s\end{bmatrix} + B[\mathbf{v}_s] + C[\mathbf{v}_r] + \begin{bmatrix}G_1\\ G_2\end{bmatrix}\left[\mathbf{i}_s - \hat{\mathbf{i}}_s\right] \quad (5)$$

The observer matrix elements G_1 and G_2 should be assigned such that the error $\mathbf{i}_s - \hat{\mathbf{i}}_s$ converges quickly to zero while preserving the system stability. In particular, an optimal dynamic response can be ensured if the eigenvalues $p_{O,1}$ and $p_{O,2}$ of the observer state matrix:

$$A_O = \begin{bmatrix} A_{11} - G_1 & A_{12} \\ A_{21} - G_2 & A_{22} \end{bmatrix} \quad (6)$$

are imposed equal, independent from the rotor speed, real and proportional, through an overall observer gain K_G, to the DFIG high frequency pole $p_{D,HF}$ at zero speed:

$$p_{D,HF} \cong -\left(\frac{R_s}{L_{s,eq}} + f_{r,eq}\right) \quad (7)$$

which is a good approximation by excess of the effective $p_{D,HF}$ value. Therefore, by the condition:

$$p_{O,1} = p_{O,2} = p_O = -K_G\left(\frac{R_s}{L_{s,eq}} + f_{r,eq}\right) \quad (8)$$

the observer gains expressions are derived:

$$\begin{cases} G_1 = A_{11} - 2p_O \\ G_2 = A_{21} + p_O^2 / A_{12} \end{cases} \quad (9)$$

In the context of a sensorless control, the space vector of the rotor voltage $\mathbf{v}_r$, which, together with $\mathbf{v}_s$ and $\mathbf{i}_s$, belongs to the input vector of the dynamical system (5), cannot be directly measured, since it is related to the actual space vector voltage $\mathbf{v}_r^{(r)}$ provided by the rotor power converter through the relation:

$$\mathbf{v}_r = \mathbf{v}_r^{(r)}\, e^{j\vartheta_e} \quad (10)$$

where:

$$\vartheta_e = p\,\vartheta_r \tag{11}$$

represents the electrical rotor position, ϑ_r the mechanical one and p the pole-pairs number. Consequently, the space vector of the rotor voltage in the stator reference frame has to be estimated by properly exploiting the observer outputs.

Since the actual $\mathbf{i}_r$ is linked through ϑ_e to $\mathbf{i}_r^{(r)}$, which is measurable, by the relation $\mathbf{i}_r = \mathbf{i}_r^{(r)} e^{j\theta_e}$, while the estimated one can be computed, coherently with Eq.(4), by the relation $\hat{\mathbf{i}}_r = \left(\hat{\boldsymbol{\Phi}}_s - L_s \mathbf{i}_s\right) \big/ L_m$, the rotor electrical position can be derived as:

$$e^{j\vartheta_e} = \frac{\mathbf{i}_r}{\mathbf{i}_r^{(r)}} \Rightarrow \hat{\vartheta}_e = \arg\left(\hat{\boldsymbol{\Phi}}_s - L_s \mathbf{i}_s\right) - \arg\left(\mathbf{i}_r^{(r)}\right) \tag{12}$$

Once $\hat{\theta}_e$ is known, the rotor speed can be estimated by:

$$\hat{\omega}_r = \frac{1}{p} \Im\left(\frac{d\hat{\theta}}{dt}\right) \tag{13}$$

with $\Im$ the functional associated to a properly sized Low Pass Filter (LPF), needed to dampen the oscillations resulting from the time derivative computation.

It is evident that the whole procedure is based on the machine parameter values, whose knowledge can be affected by uncertainties. Indeed, the *A*, *B* and *C* matrix of (5), together with $\mathbf{v}_r$, should formally be referred to their estimated version ($\hat{A}$, $\hat{B}$, $\hat{C}$ and $\hat{\mathbf{v}}_r$); analogously, in (12), L_s should be formally replaced by $\hat{L}_s$.

The possible parameter deviations determine naturally a rotor position estimation inaccuracy on $\hat{\vartheta}_e$. By denoting with $\Delta\vartheta_e$ be the rotor position estimation error:

$$\Delta\vartheta_e = \vartheta_e - \hat{\vartheta}_e \tag{14}$$

the rotor voltage $\mathbf{v}_r$ can be written as:

$$\mathbf{v}_r = \mathbf{v}_r^{(r)} e^{j\left(\hat{\vartheta}_e + \Delta\vartheta_e\right)} = \mathbf{v}_r^{(r)} e^{j\hat{\vartheta}_e} e^{j\Delta\vartheta_e} = \hat{\mathbf{v}}_r e^{j\Delta\vartheta_e} \tag{15}$$

where $\hat{\mathbf{v}}_r = \mathbf{v}_r^{(r)} e^{j\hat{\vartheta}_e}$ is the estimation of the rotor voltage in the stator reference frame. This simple relation states that the rotor voltage projection error can be compensated once a procedure to identify $\Delta\vartheta_e$ is envisioned. By denoting with $\Delta\hat{\vartheta}_e$ the estimation of $\Delta\vartheta_e$, the following approximation can be assumed for small values of $\Delta\hat{\vartheta}_e$:

$$e^{j\Delta\hat{\vartheta}_e} = \cos\Delta\hat{\vartheta}_e + j\sin\Delta\hat{\vartheta}_e \cong 1 + j\Delta\hat{\vartheta}_e \tag{16}$$

Thus, considering that the machine parameter values, as well as the rotor speed, can be affected by uncertainties, in lights of (15), and with the approximation (16), the model (5) becomes:

$$\frac{\mathrm{d}}{\mathrm{d}t}\begin{bmatrix}\hat{\mathbf{i}}_s \\ \hat{\boldsymbol{\Phi}}_s\end{bmatrix} = \hat{A}\begin{bmatrix}\hat{\mathbf{i}}_s \\ \hat{\boldsymbol{\Phi}}_s\end{bmatrix} + \hat{B}\left[\mathbf{v}_s\right] + \hat{C}\left(1 + j\Delta\hat{\vartheta}_e\right)\left[\hat{\mathbf{v}}_r\right] + G\left[\mathbf{e}\right] \tag{17}$$

where $G = \begin{bmatrix} G_1 & G_2 \end{bmatrix}^T$ and $\mathbf{e} = \mathbf{i}_s - \hat{\mathbf{i}}_s$.

In (17) the quantity $\Delta\hat{\vartheta}_e$ can be regarded as an additional machine parameter. In particular, based on the Lyapunov theory, the following adaptive law is considered:

$$\Delta\hat{\vartheta}_e = K_{\Delta\vartheta} \int_0^t \left(\hat{v}_{ry} e_x - \hat{v}_{rx} e_y\right) dt + \Delta\hat{\vartheta}_{e0} \tag{18}$$

where $K_{\Delta\vartheta}$ is a not negative number.

In presence of possible parameter deviations, the proposed adaptive observer, which is formally defined by (17), (12), (13) and (18), provides the estimation of the rotor speed $\hat{\omega}_r$ and position $\hat{\vartheta}_e$ and, moreover, is capable to track the rotor position estimation error $\Delta\hat{\vartheta}_e$.

V. Control Scheme

The whole control diagram is shown in Fig. 2. It is based on a traditional stator flux based FOC driven by the proposed sensorless adaptive observer.

In particular, by denoting with $\hat{\psi}$ the estimated angle of the stator flux provided by the observer:

$$\hat{\psi} = \arg\left(\hat{\boldsymbol{\Phi}}_s\right) \tag{19}$$

the measured rotor current space vector $\mathbf{i}_r^{(r)} = i_{r\alpha} + j i_{r\beta}$ is reported to the *dq* reference frame synchronous with $\hat{\boldsymbol{\Phi}}_s$:

$$\mathbf{i}_r^{(\Phi)} = \mathbf{i}_r^{(r)} e^{j\left(\hat{\vartheta}_e + \Delta\hat{\vartheta}_e\right)} e^{-j\hat{\psi}} = i_{rd} + j i_{rq} \tag{20}$$

and then processed by two decoupled PI regulators with outputs $\tilde{v}_{rd}, \tilde{v}_{rq}$ acting on the errors between i_{rd}, i_{rq} and their references i_{rd}^*, i_{rq}^*.

Ideally, i_{rd}^* should be set to zero and i_{rq}^* should be made proportional to the reference torque T_e^* by the torque constant K_T. However, in order to ensure an effective tracking of ϑ_e and $\Delta\vartheta_e$ in all operating conditions, an injection strategy has been implemented:

$$\begin{cases} i_{rd}^* = i_{rd,inj}^* \\ i_{rq}^* = K_T T_e^* + i_{rq,inj}^* \end{cases} \tag{21}$$

where:

$$\begin{cases} i_{rd,inj}^* = \lambda_d A_{inj} \cos\left(2\pi f_{inj} t\right) \\ i_{rq,inj}^* = K_T T_e^* + \lambda_q A_{inj} \cos\left(2\pi f_{inj} t\right) \end{cases} \tag{22}$$

with A_{inj}, f_{inj} the amplitude, frequency of the injected currents components. λ_d, λ_q (which can assume either 0 or 1 values) activate/deactivate the injection on the correspondent axis based on the DFIG operating conditions (written for sake of simplicity in *C* language style):

$$\begin{cases} \lambda_d = \left| p\omega_r - \omega \right| < \Delta\omega_{inj} \quad \| \quad \left| T_e^* \right| < \Delta T_{e,inj} \\ \lambda_q = \left| T_e^* \right| < \Delta T_{e,inj} \end{cases} \tag{23}$$

with $\Delta\omega_{inj}$ $\left(\Delta T_{e,inj}\right)$ the speed (torque) injection activation threshold.

The PI outputs $\tilde{v}_{rd}, \tilde{v}_{rq}$ are then compensated in order to carry out the decoupling action:

$$\begin{aligned} v_{rd}^* &= \tilde{v}_{rd} - \hat{\omega}_\sigma L_{s,eq} i_{rq} \\ v_{rq}^* &= \tilde{v}_{rq} + \hat{\omega}_\sigma L_{s,eq} i_{rd} + \hat{\omega}_\sigma \Phi_{s,R} \end{aligned} \tag{24}$$

with $\hat{\omega}_\sigma = \omega - p\hat{\omega}_r$ the estimated rotor slip angular frequency and $\Phi_{s,R}$ the rated stator flux. Finally, the voltage reference $v_r^{*(r)}$, which drives the rotor converter modulation, is computed as:

$$v_r^{*(r)} = v_r^{*(\Phi)} e^{-j\left(\hat{\vartheta}_e + \Delta\hat{\vartheta}_e\right)} e^{j\hat{\psi}} = v_{r\alpha}^* + j v_{rq}^* \tag{25}$$

$v_r^{*(r)}$ is also reported to the observer by the relation:

$$\hat{\mathbf{v}}_r = v_r^{*(r)} e^{j\hat{\vartheta}_e} \tag{26}$$

which effectively closes the loop on which the proposed adaptive law operates.

VI. Numerical Validation

The proposed adaptive observer has been validated through an extensive numerical analysis performed in MATLAB® Simulink® environment. The main DFIG parameters are shown in Table I, while the main algorithm quantities are reported in Table II.

TABLE I
DFIG Parameters

Variable	Symbol	Value
Rated Power	P_R	11 kW
Rated Stator Voltage	$V_{s,R}$	400 V
Rated Rotor Voltage	$V_{r,R}$	260 V
Rated Stator Frequency	$f_{s,R}$	50 Hz

TABLE II
Controller Parameters

Variable	Symbol	Value
Sampling Frequency	f_S	4 kHz
Observer Gain	K_G	5
Adaptive Law Gain	$K_{\Delta\vartheta}$	0.3 A^{-2}
Injection Current Amplitude	A_{inj}	6 %
Injection Current Frequency	f_{inj}	400 Hz

In order to test the effectiveness of the discussed adaptive law in a wide cases scenario, the electrical machine has been driven with a rotor speed assumed constant at 0.5 p.u., 1 p.u. and 1.5 p.u. in the time intervals (0 s, 6 s), (12 s, 18 s) and (24 s, 30 s) and linearly increasing in the remaining time intervals. Analogously, the reference torque has been forced to a piecewise linear behaviour, with upward steps from 0.5 p.u. to 1 p.u. at 2 s, 14 s and 26 s and downward steps from 1 p.u. to 0.5 p.u. at 4 s, 16 s and 28 s. Moreover, an error of 20% has been assumed on the flux linkage inductance.

The results of the whole simulation are shown in Fig. 3. From the *Electric Torque* and the *Rotor Speed* plots it can be noted how, in each operating condition, the algorithm is able to track the reference torque with excellent accuracy, while guarantying a negligible error between the actual rotor speed and estimated one.

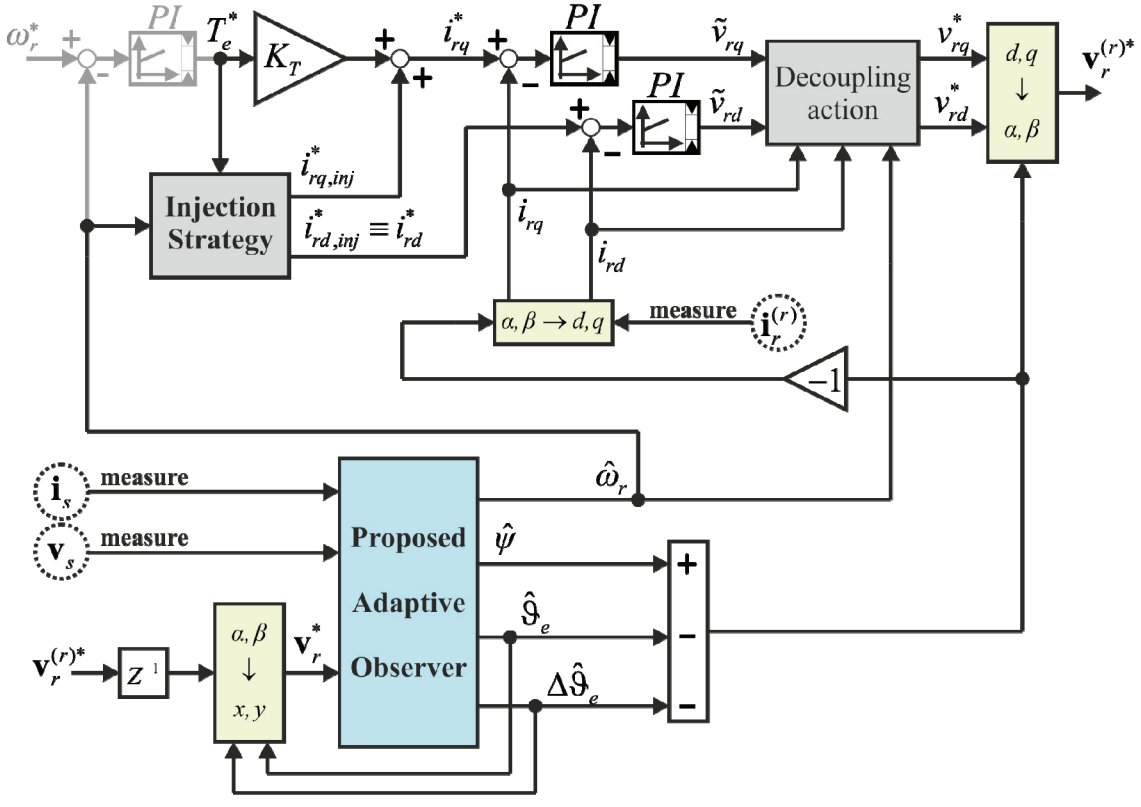

Fig. 2. Control diagram

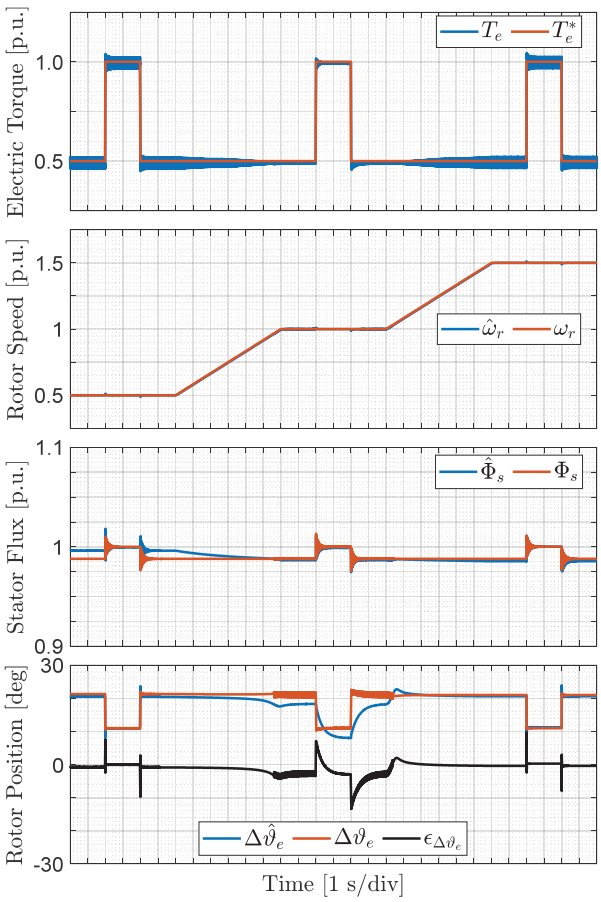

Fig. 3. System response in the whole simulation interval.

In particular, the torque behaviour highlights how the switching ripple decreases as the actual rotor speed approaches the synchronous one. This result is coherent with the corresponding rotor converter modulation index, which, indeed, decreases with the rotor frequency. The *Stator Flux* plot confirms the good performance of the system, with an associated maximum error between the modules of the actual flux and the estimated one of around 1%. It should be noted that a substantial error can be appreciated only in the low speed region, coherently with the attended observer performance, which deteriorates as the rotor speed decreases. Finally, the bottom plot depicts the behaviors of the actual and the estimated error between the measured electric rotor position and the computed one. It can be deduced that the proposed adaptive law, even in presence of strong parameters errors, is able to track effectively the steady state position error, which, in particular, never exceeds 3 deg. Conversely, the dynamic performance strongly depends on the operating condition. Indeed, while the time response of the adaptive low is quite fast in correspondence of low and high speed operations (0.5 p.u. and 1.5. p.u.), the position error convergence time assumes substantial higher values at medium speed (1 p.u.). This behaviour depends on the significantly decreased sensibility of the current errors $\mathbf{i}_s - \hat{\mathbf{i}}_s$ with respect to the position error $\Delta\vartheta_e$, which, indeed, when the rotor speed is near the synchronous one, drives the observer estimated currents though a set of rotor voltages characterized by a smaller amplitude.

The steady state behaviors of first and second phase stator and rotor currents (referred to the stator windings) at the rated torque are shown in Fig. 4. It can be noted how the results relative to low speed and high speed

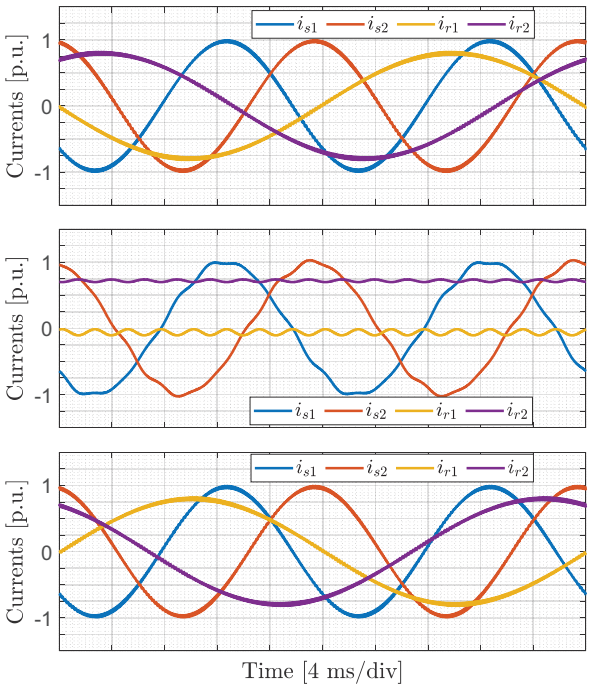

Fig. 4. Steady state behaviors.

conditions (respectively top and bottom plot) are very similar. As expected, the rotor currents frequency is half the stator one, being the correspondent rotor speeds 0.5 and 1.5 the synchronous one, while their amplitude is smaller than the stator currents one, being the correspondent direct reference components set to zero by the controller. Conversely, in correspondence of the medium speed operating condition (middle plot), the currents show the superimposed injection needed to increase tracking accuracy of the rotor position error. In particular, the stator currents become distorted and unsymmetrical, while the rotor currents (which, ideally, should be constant, being the rotor speed equal to the synchronous one) are instead characterized by a ripple at the injection frequency.

Finally, Table III compares the maximum observed $\varepsilon_{\Delta\vartheta_e}$ obtained with the proposed adaptive law (AL column) to the one associated with a conventional full

TABLE III
MAXIMUM ROTOR POSITION ERROR

Parameter Error	$\varepsilon_{\Delta\vartheta_e}$ (AL)	$\varepsilon_{\Delta\vartheta_e}$ (NAL)
+20% on L_m	1.7 deg	34 deg
+10% on L_m	0.9 deg	18 deg
-10% on L_m	0.9 deg	21 deg
-20% on L_m	2.5 deg	51 deg
+20% on $L_{\sigma s}$	≈0	5 deg
+10% on $L_{\sigma s}$	≈0	2.5 deg
-10% on $L_{\sigma s}$	≈0	3 deg
-20% on $L_{\sigma s}$	≈0	8 deg

order observer (NAL column).

VII. Conclusion

In the paper a novel adaptive sensorless full order observer for a DFIG system driven by a wind turbine has been presented. The proposed observer is based on a properly designed full order one rearranged in order to expose the rotor position error as a machine parameter. This aspect has been exploited by the formulation of an effective adaptive law allowing to track the rotor position error, which, therefore, can be used to ideally cancel the difference between the estimated position and the actual one. The developed sensorless strategy, coupled with a stator flux-based FOC, has been numerically validated in MATLAB® Simulink® environment. The simulation results confirm the effectiveness of the sensorless adaptive observer which, indeed, is able to guarantee the accuracy of the rotor position estimation even in presence of strong parameters deviation (up to ± 20%).

References

[1] Carpinelli, G., Rizzo, R., Caramia, P., Varilone, P. "Taguchi's method for probabilistic three-phase power flow of unbalanced distribution systems with correlated Wind and Photovoltaic Generation Systems" (2018) Renewable Energy, 117, pp. 227-241.

[2] R. Cardenas, R. Pena, S. Alepuz and G. Asher, "Overview of Control Systems for the Operation of DFIGs in Wind Energy Applications," in *IEEE Transactions on Industrial Electronics*, vol. 60, no. 7, pp. 2776-2798, July 2013.

[3] W. Qiao, W. Zhou, J. M. Aller and R. G. Harley, "Wind Speed Estimation Based Sensorless Output Maximization Control for a Wind Turbine Driving a DFIG," in *IEEE Transactions on Power Electronics*, vol. 23, no. 3, pp. 1156-1169, May 2008.

[4] M. K. Malakar, P. Tripathy and S. Krishnaswamy, "A predictor-corrector based rotor slip-position estimation technique for a DFIG," 2017 7th International Conference on Power Systems (ICPS), Pune, 2017, pp. 424-429.

[5] E. L. Soares, F. V. Rocha, L. M. S. de Siqueira and N. Rocha, "Sensorless Rotor Position Detection of Doubly-Fed Induction Generators for Wind Energy Applications," 2018 13th IEEE International Conference on Industry Applications (INDUSCON), São Paulo, Brazil, 2018, pp. 1045-1050.

[6] M. Abdelrahem, C. Hackl and R. Kennel, "Sensorless control of doubly-fed induction generators in variable-speed wind turbine systems," 2015 International Conference on Clean Electrical Power (ICCEP), Taormina, 2015, pp. 406-413.

[7] D. D. Reigosa, F. Briz, C. Blanco Charro, A. Di Gioia, P. García and J. M. Guerrero, "Sensorless Control of Doubly Fed Induction Generators Based on Rotor High-Frequency Signal Injection," in IEEE Transactions on Industry Applications, vol. 49, no. 6, pp. 2593-2601, Nov.-Dec. 2013.

[8] L. Xu, E. Inoa, Y. Liu and B. Guan, "A New High-Frequency Injection Method for Sensorless Control of Doubly Fed Induction Machines," in IEEE Transactions on Industry Applications, vol. 48, no. 5, pp. 1556-1564, Sept.-Oct. 2012.

[9] R. Cardenas, R. Pena, J. Proboste, G. Asher, J. Clare and P. Wheeler, "MRAS Observers for sensorless control of doubly-fed induction generators," 2008 4th IET Conference on Power Electronics, Machines and Drives, York, 2008, pp. 568-572.

[10] M. Pattnaik and D. Kastha, "Adaptive speed observer for a stand-alone doubly fed induction generator feeding nonlinear and unbalanced loads," 2013 IEEE Power & Energy Society General Meeting, Vancouver, BC, 2013, pp. 1-1.

[11] R. Bhattarai, N. Gurung, A. Thakallapelli and S. Kamalasadan, "Reduced-Order State Observer-Based Feedback Control Methodologies for Doubly Fed Induction Machine," in IEEE Transactions on Industry Applications, vol. 54, no. 3, pp. 2845-2856, May-June 2018.

[12] D. G. Forchetti, G. O. Garcia and M. I. Valla, "Adaptive Observer for Sensorless Control of Stand-Alone Doubly Fed Induction Generator," in IEEE Transactions on Industrial Electronics, vol. 56, no. 10, pp. 4174-4180, Oct. 2009.

[13] S. Yang and V. Ajjarapu, "A Speed-Adaptive Reduced-Order Observer for Sensorless Vector Control of Doubly Fed Induction Generator-Based Variable-Speed Wind Turbines," in IEEE Transactions on Energy Conversion, vol. 25, no. 3, pp. 891-900, Sept. 2010.

[14] S. Mondal and D. Kastha, "Improved Direct Torque and Reactive Power Control of a Matrix-Converter-Fed Grid-Connected Doubly Fed Induction Generator," in IEEE Transactions on Industrial Electronics, vol. 62, no. 12, pp. 7590-7598, Dec. 2015.

[15] J. Arbi, M. J. Ghorbal, I. Slama-Belkhodja and L. Charaabi, "Direct Virtual Torque Control for Doubly Fed Induction Generator Grid Connection," in IEEE Transactions on Industrial Electronics, vol. 56, no. 10, pp. 4163-4173, Oct. 2009.

[16] J. Hu, J. Zhu, Y. Zhang, G. Platt, Q. Ma and D. G. Dorrell, "Predictive Direct Virtual Torque and Power Control of Doubly Fed Induction Generators for Fast and Smooth Grid Synchronization and Flexible Power Regulation," in IEEE Transactions on Power Electronics, vol. 28, no. 7, pp. 3182-3194, July 2013.

[17] N. Amiri, S. M. Madani, T. A. Lipo and H. A. Zarchi, "An Improved Direct Decoupled Power Control of Doubly Fed Induction Machine Without Rotor Position Sensor and With Robustness to Parameter Variation," in IEEE Transactions on Energy Conversion, vol. 27, no. 4, pp. 873-884, Dec. 2012.

[18] G. Abad, M. Á. Rodriguez and J. Poza, "Three-Level NPC Converter-Based Predictive Direct Power Control of the Doubly Fed Induction Machine at Low Constant Switching Frequency," in IEEE Transactions on Industrial Electronics, vol. 55, no. 12, pp. 4417-4429, Dec. 2008.